Exploring the Molecular Mechanism for Color Distinction in Humans

Rene J. Trabanino,[†] Nagarajan Vaidehi,[‡] and William A. Goddard, III*

Materials and Process Simulation Center (139-74), California Institute of Technology, Pasadena, California 91125

Received: December 8, 2005; In Final Form: May 4, 2006

We examine here the role of the red, green, and blue human opsin structures in modulating the absorption properties of 11-*cis*-retinal bonded to the protein via a protonated Schiff base (PSB). We built the three-dimensional structures of the human red, green, and blue opsins using homology modeling techniques with the crystal structure of bovine rhodopsin as the template. We then used quantum mechanics (QM) combined with molecular mechanics (MM) (denoted as QM/MM) techniques in conjunction with molecular dynamics to determine how the room temperature molecular structures of the three human color opsin proteins modulate the absorption frequency of the same bound 11-*cis*-retinal chromophore to account for the differences in the observed absorption spectra. We find that the conformational twisting of the 11-*cis*-retinal PSB plays an important role in the green to blue opsin shift, whereas the dipolar side chains in the binding pocket play a surprising role of red-shifting the blue opsin with respect to the green opsin, as a fine adjustment to the opsin shift. The dipolar side chains play a large role in the opsin shift from red to green.

1. Introduction

Color vision in humans is based on a single chromophore, 11-*cis*-retinal, bound covalently to the red, green, and blue opsin G-protein-coupled receptors (GPCRs) in such a way as to provide selective responses to the red, green, and blue parts of the visible spectrum.[1] Our interest here is to understand the molecular basis of the color distinction in terms of how 11-*cis*-retinal interacts with the three opsin proteins to modulate its absorption frequency.

11-*cis*-Retinal absorbs radiation at a wavelength maximum of ∼380 nm in organic solvents such as ethanol,[2] but at physiologic pH the protonated Schiff base (PSB) form of 11-*cis*-retinal (outside the protein) shifts the absorption frequency to a maximum at 440 nm.[1] When 11-*cis*-retinal forms a Schiff base/opsin protein complex (as shown in Figure 1), the residues in the binding site of 11-*cis*-retinal in the three opsin proteins modulate further the absorption frequency. Thus, the opsin/retinal complex in the rod cells of the eye (where rhodopsin is localized) absorbs light at ∼500 nm.[3] The cone cells in humans contain three types of opsins, which allow retinal to absorb light maximally in the blue (∼425 nm), green (∼530 nm), and red (∼560 nm) regions of the visible spectrum.[1]

In this paper we examine the molecular factors that tune the absorption frequency of 11-*cis*-retinal. Factors that might be expected to contribute to the spectral shift (shift in absorption frequency between free and protein-bound retinal) in opsins include the (1) degree to which the polyene chain of the retinal is coplanar with the ionone ring,[4] (2) interaction of the retinal Schiff base with its counterion (acidic side chain),[5] (3) influence of charged and dipolar residues near the retinal conjugated system,[6] and (4) effect of polarizable side chains (such as aromatic side chains) near the retinal conjugated system.[3]

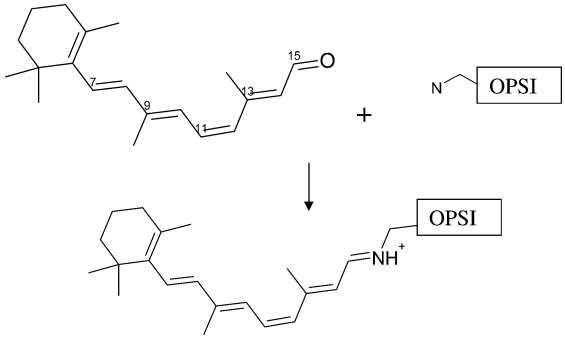

Figure 1. A schematic of the Schiff base bond formation of retinal to a lysine side chain in the opsin protein. The ring is referred to as the ionone ring.

The retinal coplanarity was studied in bacteriorhodopsin (bR) by using retinal analogues having the ionone ring "locked", preventing it from twisting.[4] This analogue locks the C6−C7 bond adjacent to the ionone ring, which is known to modulate spectroscopic properties of the protein/retinal complex.[7] The spectral red shift due to twisting of this ionone ring was found to be ∼1200 cm^{-1} to the red (out of the total 5100 cm^{-1} red shift for bR).

To understand how factors 2, 3, and 4 may cause spectral shifts, it is useful to consider the resonance structures of the protonated and deprotonated 11-*cis*-retinal Schiff bases (Figure 2). Two important facts confirmed by experiment and theory[8,9] in relation to these structures are (a) the excited-state wave function has a larger weight on the right-hand resonance structures than the ground state and (b) the excited state has a more delocalized wave function with less double bond alternation than the ground state.

Experiments suggest that the excited state of 11-*cis*-retinal has an experimental dipole moment of 23.0 D (considered an upper limit value), which is 2.2 times larger than that of the ground state (10.3 D).[8] This led to the proposition that, upon excitation, the positive charge moves toward the ionone ring.

* To whom correspondence should be addressed. E-mail: wag@wag.caltech.edu.
[†] Current address: UCLA School of Medicine, Los Angeles, CA 90095.
[‡] Current address: Division of Immunology, Beckman Research Institute of City of Hope, Duarte, CA 91010.

10.1021/jp057144q CCC: $33.50
Published on Web 07/29/2006

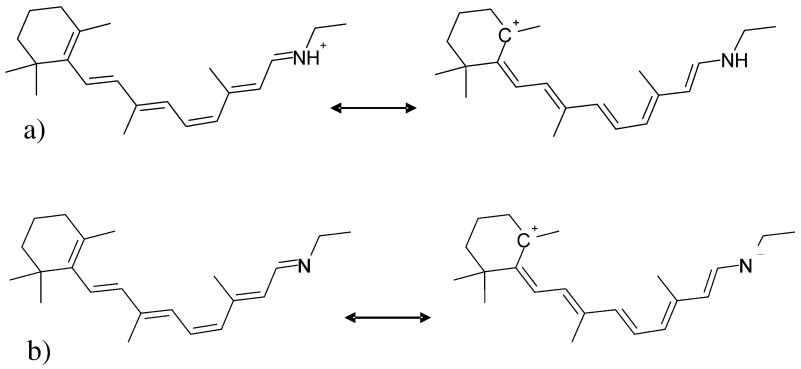

Figure 2. Resonance structures for the (a) protonated Schiff base and (b) deprotonated Schiff base of retinal. Experiment and theory[1,2] have shown that the dipole moment of this Schiff base increases on excitation and concurrently there is more weight to the right-side structures in the calculated excited-state wave functions.

In addition, the relative stability of these structures, and thus the excitation energy, may be influenced by a permanent electric field (or a polarizable medium) in the environment of the chromophore.[3,9]

Our calculations for 11-*cis*-retinal indicate a more modest increase in dipole moment from 5.6 to 6.9 D [from the ground to the excited triplet state, as calculated with Hartree−Fock (HF) quantum mechanics (QM)[10]]. Similarly, in the case of the protonated Schiff base of retinal (with a chloride counterion), the experimental dipole change is from 6 to 18 D[8] as compared to the more modest increase (from 13.8 to 16.4 D) by our QM calculations.

The role of the charged or dipolar residues in the frequency modulations has long been studied, notably by Spudich et al.[11] On the basis of experiments with retinal analogues and π-electron calculations (in phototaxis receptor sensory rhodopsin and bacteriorhodopsin), they proposed an external point charge model for the opsin bathochromic shift as including a counterion in the proximity of the Schiff base, as well as an ion pair near the ionone ring. The role of the Schiff base counterion was also explored by Sakmar et al. The role of the counterion was tested by mutating Glu113 on TM3 in bovine rhodopsin to Asp, Gln, Asn, and Ala.[5] The last three mutations led to a reduction in the pK_a of the Schiff base (to 6.00, 6.71, and 5.70, respectively) and also to a decrease in the excitation energy (shift to 496, 520, and 506 nm in the absorption maxima) due to the role of the negatively charged counterion in stabilizing the charge distribution of the ground state (which is more positive near the Schiff base region) and destabilizing the excited state (which is more negative around the Schiff base region). The role of the dipolar binding site residues in the other opsins was studied by Kochendoerfer et al.[1] Using resonance Raman spectroscopy on the opsin/retinal complexes, they found that the peak for the ethylenic stretch gradually shifted (blue, 1559 cm^{-1}, to green, 1531 cm^{-1}, to red, 1526 cm^{-1}) over the three opsins. This is believed to result from the increasing electronic delocalization in the red opsin environment (and concomitant reduction in bond alternation). On the basis of model structures of the human opsins, they found that the distribution of dipolar residues around the ionone ring increased from the blue to the red opsin. Qualitatively, these residues lead to differential stabilization of the ground- and excited-state electron distributions in much the same way as does the counterion.

The effect of the polarizable side chains (such as aromatic side chains) around the retinal conjugated system was studied (in bacteriorhodopsin) by Houjou et al.[3] using the quantum mechanics with a self-consistent reaction field (SCRF). Here the charge distribution of the retinal polarizes the medium, which in turn produces a reaction field which acts back on the retinal. The calculated bacteriorhodopsin shift arising from the effect of the polarizable medium was ∼1000 cm^{-1}. However, the polarizable medium was uniform and thus did not simulate actual aromatic side chains in the vicinity of retinal. In addition, he did not include the effect of dipolar residues in his calculations.

Rajamani et al.[12] used semiempirical QM/molecular mechanics (MM), Monte Carlo sampling, and molecular dynamics (MD) to explain the opsin shift from 6-*s*-*cis*-PSB (in methanol with solvation) to 6-*s*-*cis*-PSB (in a vacuum) to 6-*s*-*trans*-PSB (in a vacuum) to 6-*s*-*trans*-PSB (in bacteriorhodopsin). Some of the contributions to the opsin shift were found (1800 cm^{-1} for the differential solvatochromic effect between the solution and protein, 2400 cm^{-1} for the rotation about the 6-*s* bond with extension of the π-system). This study did not calculate the effect of the polarizable residues in the protein and used a semiempirical method for the determination of excited states. In the current study, we employed QM/MM/MD to determine the opsin shifts in a photoexcitation system. However, we focused on the relative shifts across human opsin proteins using ab initio methods for determining the excited states.

Damjanovic et al.[13] used molecular dynamics to generate various conformations of the bacterial light-harvesting complex II. Ab initio HF/CIS calculations were performed on these conformations; these results were then used to construct a time-dependent Hamiltonian, which was used to generate an absorption spectrum using linear response theory. This rigorous approach to this system allowed the authors to obtain highly accurate absorption spectra. Nevertheless, in the study it was not attempted to understand the various environmental factors responsible for shifting the excitation energy.

The more recent determination of the crystal structure for bovine rhodopsin[14] reveals the specific residues in the binding site of 11-*cis*-retinal that might be involved in spectral tuning among the three human opsins. The sequence identities (similarities) between bovine rhodopsin and the human opsins are as follows: 88% (91%) human rhodopsin, 40% (60%) human blue opsin, 40% (57%) human green opsin, 39% (56%) human red opsin. The identities of bovine rhodopsin and the human opsins in the TM core regions (as previously described[15]) only are (blue) 43%, (green) 41%, and (red) 38%. This high similarity justifies the use of homology modeling and threading techniques to determine the opsin structures.[16] On the basis of the structures of the three opsins built using homology modeling techniques from the crystal structure of bovine rhodopsin, we analyzed systematically the components of the opsin shift. Since the computational costs of such QM calculations increase rapidly

```
gi|129204|sp|P02699|OPSD_BOVIN      ------------------MNGTEGPNFYVPFSNKTGVVRSPFEAPQYYLA
gi|129207|sp|P08100|OPSD_HUMAN      ------------------MNGTEGPNFYVPFSNATGVVRSPFEYPQYYLA
gi|129215|sp|P04001|OPSG_HUMAN      MAQQWSLQRLAGRHPQDSYEDSTQSSIFTYTNS--NSTRGPFEGPNYHIA
gi|129219|sp|P04000|OPSR_HUMAN      MAQQWSLQRLAGRHPQDSYEDSTQSSIFTYTNS--NSTRGPFEGPNYHIA
gi|129203|sp|P03999|OPSB_HUMAN      ------------------MRKMSEEEFYLFKN---ISSVGPWDGPQYHIA
                                                      .     .::   .       .*:: *:*::*

gi|129204|sp|P02699|OPSD_BOVIN      EPWQFSMLAAYMFLLIMLGFPINFLTLYVTVQHKKLRTPLNYILLNLAVA
gi|129207|sp|P08100|OPSD_HUMAN      EPWQFSMLAAYMFLLIVLGFPINFLTLYVTVQHKKLRTPLNYILLNLAVA
gi|129215|sp|P04001|OPSG_HUMAN      PRWVYHLTSVWMIFVVIASVFTNGLVLAATMKFKKLRHPLNWILVNLAVA
gi|129219|sp|P04000|OPSR_HUMAN      PRWVYHLTSVWMIFVVTASVFTNGLVLAATMKFKKLRHPLNWILVNLAVA
gi|129203|sp|P03999|OPSB_HUMAN      PVWAFYLQAAFMGTVFLIGFPLNAMVLVATLRYKKLRQPLNYILVNVSFG
                                      * : : :.:*  :.  ..  * :.* .*::.**** ***:**:*::..

gi|129204|sp|P02699|OPSD_BOVIN      DLFMVFGGFTTTLYTSLHGYFVFGPTGCNLEGFFATLGGEIALWSLVVLA
gi|129207|sp|P08100|OPSD_HUMAN      DLFMVLGGFTSTLYTSLHGYFVFGPTGCNLEGFFATLGGEIALWSLVVLA
gi|129215|sp|P04001|OPSG_HUMAN      DLAETVIASTISVVNQVYGYFVLGHPMCVLEGYTVSLCGITGLWSLAIIS
gi|129219|sp|P04000|OPSR_HUMAN      DLAETVIASTISIVNQVSGYFVLGHPMCVLEGYTVSLCGITGLWSLAIIS
gi|129203|sp|P03999|OPSB_HUMAN      GFLLCIFSVFPVFVASCNGYFVFGRHVCALEGFLGTVAGLVTGWSLAFLA
                                    .:   . .    .  .  ****:*   * ***:  :: *    ***..::

gi|129204|sp|P02699|OPSD_BOVIN      IERYVVVCKPMSNFRFGENHAIMGVAFTWVMALACAAPPLVGWSRYIPEG
gi|129207|sp|P08100|OPSD_HUMAN      IERYVVVCKPMSNFRFGENHAIMGVAFTWVMALACAAPPLAGWSRYIPEG
gi|129215|sp|P04001|OPSG_HUMAN      WERWMVVCKPFGNVRFDAKLAIVGIAFSWIWAAVWTAPPIFGWSRYWPHG
gi|129219|sp|P04000|OPSR_HUMAN      WERWLVVCKPFGNVRFDAKLAIVGIAFSWIWSAVWTAPPIFGWSRYWPHG
gi|129203|sp|P03999|OPSB_HUMAN      FERYIVICKPFGNFRFSSKHALTVVLATWTIGIGVSIPPFFGWSRFIPEG
                                     **::*:***:.*.**. : *:  :  :*  .   : **: ****: *.*

gi|129204|sp|P02699|OPSD_BOVIN      MQCSCGIDYYTPHEETNNESFVIYMFVVHFIIPLIVIFFCYGQLVFTVKE
gi|129207|sp|P08100|OPSD_HUMAN      LQCSCGIDYYTLKPEVNNESFVIYMFVVHFTIPMIIIFFCYGQLVFTVKE
gi|129215|sp|P04001|OPSG_HUMAN      LKTSCGPDVFSGSSYPGVQSYMIVLMVTCCITPLSIIVLCYLQVWLAIRA
gi|129219|sp|P04000|OPSR_HUMAN      LKTSCGPDVFSGSSYPGVQSYMIVLMVTCCIIPLAIIMLCYLQVWLAIRA
gi|129203|sp|P03999|OPSB_HUMAN      LQCSCGPDWYTVGTKYRSESYTWFLFIFCFIVPLSLICFSYTQLLRALKA
                                    :: *** * ::       :*:   :::     *: :* :.* *:  :::

gi|129204|sp|P02699|OPSD_BOVIN      AAAQQQESATTQKAEKEVTRMVIIMVIAFLICWLPYAGVAFYIFTHQGSD
gi|129207|sp|P08100|OPSD_HUMAN      AAAQQQESATTQKAEKEVTRMVIIMVIAFLICWVPYASVAFYIFTHQGSN
gi|129215|sp|P04001|OPSG_HUMAN      VAKQQKESESTQKAEKEVTRMVVVMVLAFCFCWGPYAFFACFAAANPGYP
gi|129219|sp|P04000|OPSR_HUMAN      VAKQQKESESTQKAEKEVTRMVVVMIFAYCVCWGPYTFFACFAAANPGYA
gi|129203|sp|P03999|OPSB_HUMAN      VAAQQQESATTQKAEREVSRMVVVMVGSFCVCYVPYAAFAMYMVNNRNHG
                                    .* **:** :*****:**:***::*: :: .*: **: .* :   : .

gi|129204|sp|P02699|OPSD_BOVIN      FGPIFMTIPAFFAKTSAVYNPVIYIMMNKQFRNCMVTTLCCGKNPLGDDE
gi|129207|sp|P08100|OPSD_HUMAN      FGPIFMTIPAFFAKSAAIYNPVIYIMMNKQFRNCMLTTICCGKNPLGDDE
gi|129215|sp|P04001|OPSG_HUMAN      FHPLMAALPAFFAKSATIYNPVIYVFMNRQFRNCILQLF-GKKVDDGSEL
gi|129219|sp|P04000|OPSR_HUMAN      FHPLMAALPAYFAKSATIYNPVIYVFMNRQFRNCILQLF-GKKVDDGSEL
gi|129203|sp|P03999|OPSB_HUMAN      LDLRLVTIPSFFSKSACIYNPIIYCFMNKQFQACIMKMVCGKAMTDESDT
                                    :   : ::*::*:*:: :***:** :**:**: *::  .        .:

gi|129204|sp|P02699|OPSD_BOVIN      ASTT---VSKTETSQVAPA
gi|129207|sp|P08100|OPSD_HUMAN      ASAT---VSKTETSQVAPA
gi|129215|sp|P04001|OPSG_HUMAN      SSASKTEVSSVSS--VSPA
gi|129219|sp|P04000|OPSR_HUMAN      SSASKTEVSSVSS--VSPA
gi|129203|sp|P03999|OPSB_HUMAN      CSSQKTEVSTVSSTQVGPN
                                    .*:    **...:  *.*
```

Figure 3. Multiple-sequence alignment of the four human opsin proteins with bovine rhodopsin used for constructing the opsin structures studied here.

with the number of atoms, we used combined QM/MM or QM/MM/MD calculations treating the ground and excited states of retinal PSB (and/or selected residues) using HF QM and the protein environment using a force field (FF).

Specifically, the systematic analysis of this study is divided into four parts: (1) QM/MM on complexes with retinal PSB in the same orientation—QM on retinal PSB, FF on the protein (to obtain a contribution by the protein dipolar residues to the opsin shift); (2) QM/MM on complexes with retinal PSB in the same orientation, but with various Monte Carlo conformations of the side chain at position 265 (Trp in red and green, Tyr in blue)—QM on retinal PSB and residue 265, FF on the rest of the protein (to obtain a contribution by the polarizable residue at position 265 on the opsin shift); (3) QM/MM on complexes with both the retinal PSB and protein in various conformations generated by MD (with QM-fitted parameters)—QM on retinal PSB, FF on the protein (to obtain contributions by the retinal PSB twisting and the dipolar residues on the opsin shift); this step yielded calculated absorption spectra reflecting the room temperature variations in retinal PSB/opsin structure; (4) QM at the CIS level of theory on local residues from the MD snapshots (QM on retinal PSB, residue 265, and/or residue 113).

The goal of this study was to determine relative spectral shifts between the opsins (although absolute values for the absorption peaks were also determined, they are less accurate than relative shifts using the HF QM method). As such, we found that a major contribution to the large opsin shift between the green and the blue opsins was from the twisting of the retinal PSB chain to accommodate steric effects of surrounding residues. In addition, there was a more minor yet significant role of the dipolar side chains and the polarizable groups in the opsin shift from green to blue. The remaining discrepancy between the calculated and experimental opsin shifts (from green to blue) may be partly due to electron correlation (not included in HF) and may involve the polarizable residues. Some preliminary CIS calculations indicate the role of the polarization contained in a higher level of theory. We conclude that the dipolar residues dominate the small opsin shift from the red to green opsins. In addition, the twisting of the retinal PSB chain plays an important role in the opsin shift from green to blue.

2. Methods

2.1. Opsin Structure Building. The multiple-sequence alignment (Figure 3) of the sequences for bovine rhodopsin with those of the four human opsins (rhodopsin and the three color opsins) was obtained using ClustalW.[17] On the basis of this alignment, the sequence of each human opsin was threaded through the bovine rhodopsin structural template as follows. Side chain replacement using SCWRL[18] of the bovine rhodopsin structure (PDB code 1F88) was carried out to replace those in the bovine rhodopsin structure with the correct sequence of the respective opsin. SCWRL obtains optimized rotamers for the side chain using a backbone-dependent library of rotamers. As shown in Figure 3, the only gaps in the alignment occurred in

the N and C termini. These regions with gaps were excluded from the built structures, since they are likely too distant from the bound retinal to have a significant role in spectral tuning.

The protein structure was described using the Dreiding force field[19] with charges assigned from CHARMM22.[20] The structures of the proteins were optimized in vacuum using conjugate gradient minimization (to a 0.1 (kcal/mol)/Å RMS force) as implemented in MPSim.[21] Then the retinal PSB was placed into the opsins in the same orientation as in the bovine rhodopsin crystal structure. SCWRL was performed twice (with an intermediate potential energy minimization step) to optimize side chain rotamers in the presence of the retinal PSB. A side chain replacement program called SCREAM (Kam, Vaidehi, and Goddard, manuscript in preparation), which uses an explicit potential energy calculation to score side chain rotamers, was subsequently used to finely optimize side chains in the 5 Å binding site of the retinal PSB. The retinal PSB was kept fixed in these optimizations. These opsin structures (PDB with counterions) may be found in the Supporting Information.

2.2. Quantum Mechanical Calculations on Retinal and Derivatives. To validate the accuracy of excitation energies for retinal within the opsins, we carried out HF QM calculations using the 6-31G** basis set (using Jaguar[10] software) on both the free 11-*cis*-retinal and the PSB 11-*cis*-retinal. The geometry was optimized for the ground-state (closed-shell singlet, CSS) electronic state. Then we calculated the excited triplet state (TS) keeping the ground-state geometry. This triplet-state wave function was used as an initial guess to obtain the open-shell singlet (OSS) state. The energy difference between this OSS state and the CSS state is denoted as VEE(calcd-oss) (calculated vertical excitation energy to the OSS). This leads to a VEE-(calcd-oss) corresponding to 413 nm compared to the experimental value of 380 nm. The energy difference between the TS state and the CSS state is denoted as VEE(calcd-ts) (calculated vertical excitation energy to the TS). This leads to a VEE(calcd-ts) corresponding to 428 nm compared to the experimental value of 380 nm.

2.3. QM/MM Calculation on the Opsin/Retinal Complex (Theory). To describe the effect of the protein on the absorption spectrum of retinal PSB, we used the QM/MM method of Murphy et al.[22] as implemented in Jaguar.[10] The molecular system is partitioned into a QM portion (retinal PSB and/or selected residues) and an MM portion (rest of the opsin structure). In the QM calculations the electrostatic field of the MM region (described as point charges) is included directly in the QM Hamiltonian, which effectively allows the electronic state of the QM region to be polarized by the protein environment. Within the QM region, the HF method with the 6-31G** basis set was used. The MM forces were evaluated using MPSim[21] with the Dreiding force field (using a dielectric constant of 1.0).[19] We did not include explicit solvation in this study; the protein complex was assumed to be in a vacuum with appropriate counterions for each charged residue. In addition, the retinal PSB was kept fixed in all QM/MM calculations (except the MD simulations discussed in section 2.4); the protein atoms were also kept fixed in all QM/MM calculations [except the SCREAM side chain Monte Carlo optimization of residue 265 to explore its polarizability (discussed below) and the MD simulations (discussed in section 2.4)].

The QM/MM calculations were carried out for both the ground state and the triplet excited states to obtain the VEE-(calcd-trip). In this way we determined the roles of the first three factors described in section 1.

The fourth factor as described in section 1 is expected to arise from the effect of the nearby aromatic side chains, which may polarize in response to the retinal excitation (and its subsequent increase in dipole moment). Since the side chains described with an FF are nonpolarizable, this factor is tested with QM calculations. The procedure is as follows. The QM region is chosen to be the retinal PSB together with the aromatic polarizable residue (tyrosine or tryptophan) at position 265 (bovine rhodopsin numbering) in the protein. The unpaired electrons remain on the retinal chain in the excited-state calculation in the field of a polarizable ground-state aromatic side chain. This calculation is performed both in a vacuum and in the field of an MM-treated protein environment to ascertain any additional influence the rest of the protein may have on the polarizability of the aromatic side chain. Since the HF method is used for the QM calculations, this step is expected to be the least accurate owing to the lack of explicit electron correlation. Calculations using the CIS method underscore the importance of electron correlation in extracting the polarization effect.

2.4. Molecular Dynamics Using a QM-Fitted Force Field. The dynamical fluctuations in the protein structure can shift the absorption energies, and hence, to calculate the absorption spectrum, we should account for the ensemble of structures as they are accessed in room temperature dynamics. To determine this effect using MD simulations, we first modified our FF parameters to fit closely to the structure of retinal PSB from QM calculations. We used the QM-derived (HF) values of 1.36 and 1.44 Å for alternating bond distances for the polyene chain of PSB, as well as 23 and 7 kcal/mol as the torsion barriers for these bonds. The FF charges for retinal PSB were assigned to fit the QM electrostatic potential. Using the Dreiding FF for all interactions, we minimized the retinal PSB structure without protein. We found that the minimized retinal PSB structure had a vertical excitation energy ~2 kcal/mol higher than for the QM geometry-optimized structure. The coordinate RMS difference between these structures was 0.09 Å. This justifies the use of this modified force field for our opsin shift (relative excitation energy) studies.

Subsequently, we carried out MD simulations of the 11-*cis*-retinal PSB/opsin complex (all atoms movable, except the terminal carbon of retinal PSB, to serve as an anchor to prevent the molecule from moving out of its binding pocket) for 100 ps using a Nose−Hoover temperature heat bath (TVN) at 300 K. Then single-point QM/MM energies as described above were obtained for snapshots obtained every 2 ps (50 snapshots of structures for red, green, and blue retinal PSB/opsin complexes) of the MD trajectory. This leads to absorption spectra reflective of dynamical changes in the protein and ligand.

2.5. CIS Method Applied to MD-Generated Structures. To further explore the role of the polarizable residues on the opsin shift, the snapshots obtained from MD simulation were analyzed in the following manner. The retinal PSB and residue 265 were extracted from those snapshots. These complexes were designated as local_PSB_265. In addition (to determine the role of the counterion on polarizability), the retinal PSB, residue 265, and residue 113 (Glu) were extracted from the snapshots. These complexes are designated as local_PSB_265_113.

Using Jaguar, we carried out single-point CIS calculations on the complexes obtained above. Such calculations (without the entire protein) effectively isolate the effect of residue 265 and/or residue 113 on the opsin shift. The last 40−50 snapshots were used for the CIS calculations (to represent the system after stabilization).

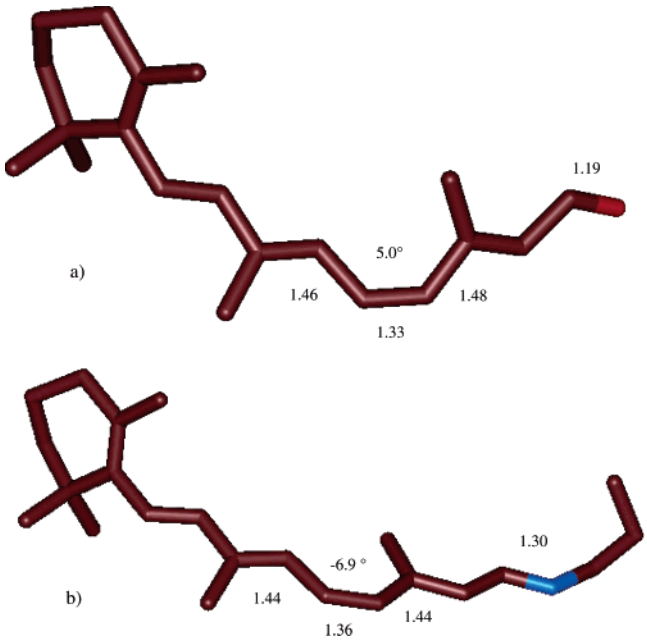

Figure 4. QM geometry-optimized structures of (a) 11-*cis*-retinal and (b) PSB retinal. Bond distances (Å) involving the 10, 11, 12, and 13 atoms and the torsion angle for the 11-*cis* bond are shown. Note that there is less bond alternation for the PSB retinal due to the higher degree of delocalization.

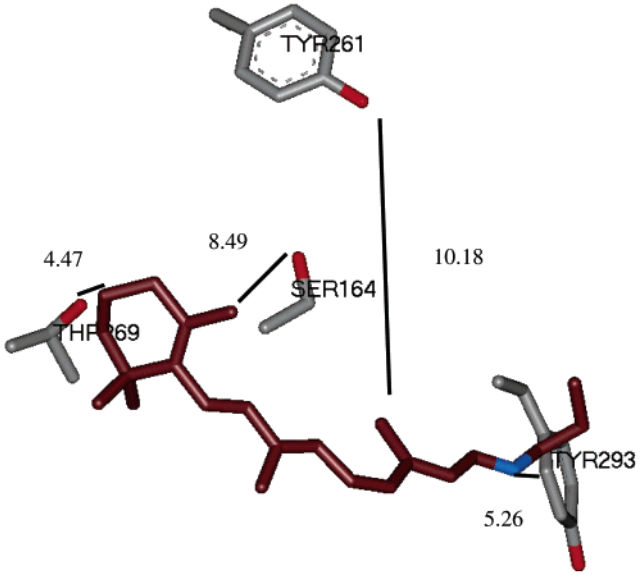

Figure 5. Dipolar residues within the vicinity of the PSB retinal in the red opsin, which are nonpolar residues in the green opsin. These are the main contributors to the opsin shift from red to green. The distances between the residues and the PSB retinal are indicated (Å).

3. Results and Discussion

3.1. QM on 11-*cis*-Retinal and Derivatives. The QM geometry-optimized (at the HF level) structure of 11-*cis*-retinal is shown in Figure 4a. Calculating the CSS and OSS energies from this geometry led to a VEE(calcd-oss) of 69.3 kcal/mol. This corresponds to a photon wavelength of 413 nm, as compared to the 380 nm determined experimentally (75.2 kcal/mol). The calculated excitation energy to the triplet state, or VEE(calcd-ts), is 66.8 kcal/mol or 428 nm. This discrepancy most likely arises from the use of HF, which does not include the electron correlation of DFT or CIS. Using CI singles (CIS), we obtain an excitation energy of 109.3 kcal/mol, much higher than with OSS or experiment. We also calculated the HF triplet, CIS singlet, and TDHF singlet excitation energies for the excited state of 11-*cis*-retinal using Turbomole,[22], leading to (HF triplet) 64.0 kcal/mol, (CIS singlet) 107.8 kcal/mol, and (TDHF singlet) 102.5 kcal/mol. These results are consistent with prior work on retinal by Lopez et al.[24] For further comparison, we also determined the excitation energy of 11-*cis*-retinal using EOM-CCSD (equation of motion coupled cluster method)[25,26] with the GAMESS[27] software, leading to an excitation energy of 99.8 kcal/mol.

Thus, there clearly is some cancellation of errors in using OSS to describe the singlet transitions for the various opsins, the objective for this study. In addition, we used the CSS to triplet transition to obtain the relative opsin shifts for retinal within the opsin protein. Again, we expect the error in this approximation to decrease for the relative VEE(calcd), as evidenced by the accuracy of our results.

The exception to the above argument is for the contribution by the polarizable residue (at position 265) of the protein on the retinal PSB electronic structure, where the lack of explicit electron correlation within the QM region may affect the relative VEE(calcd). This is because the comparison is across systems (green to blue opsin) involving different polarizable residues (thus errors need not cancel). We should clarify here that the QM region *can* be polarized by the protein in the current implementation of QM/MM (allowing the effect of the protein on the retinal PSB electronic structure to be included) and the QM subregions *may* not be polarized effectively by other QM subregions due to the lack of electron correlation in HF.

The QM geometry-optimized structure of a retinal PSB structure is shown in Figure 4b. It consists of the bound retinal and three carbons of the lysine side chain. The CSS to triplet energy is 42.9 kcal/mol (and the CSS to OSS energy is 47.7 kcal/mol). Performing a QM/MM calculation using QM to describe the PSB structure (the same conformation as above) and including the Glu113 counterion in the MM system, we obtain a CSS to triplet energy of 44.6 kcal/mol. Placing the same retinal PSB into the bovine rhodopsin crystal structure (matching the ligand orientation with that in the crystal structure) leads to a CSS to triplet energy of 43.5 kcal/mol. These relative differences indicate the role of the counterions in blue-shifting the energy gap and the role of the rest of the bovine rhodopsin protein in red-shifting from there. Later (in section 3.4), we will find that the dynamics of the ligand in the protein leads to changes in the ligand conformation in response to the protein that also modulates this energy gap.

3.2. QM/MM on Opsin Complexes. Single-point QM/MM energy calculations were carried out with the retinal PSB in the *same* conformation as above. The VEE(calcd-os) values were 43.5, 44.9, and 42.9 kcal/ mol for red, green, and blue opsins, respectively. Thus, the calculated energy gap shifts are 1.4 kcal/mol for red to green and −2.0 kcal/mol for green to blue. The experimental values for these opsin shifts are 2.9 kcal/mol for red to green and 13.3 kcal/mol for green to blue. The error of $2.9 - 1.4 = 1.5$ kcal/mol for the red−green opsin shift is most likely due to the lack of solvation within the protein as well as the assumption of a frozen complex (room temperature effects will be explored in section 3.4). More significantly, the larger discrepancy in the green−blue opsin shift points to the need for accounting for room temperature variations in structure [since the residues closest (<5 Å) to the retinal PSB are different between green and blue], which will be discussed in section 3.4.

Some important residues in the vicinity (<10 Å) of the retinal PSB in the red opsin are shown in Figure 5. These residues are

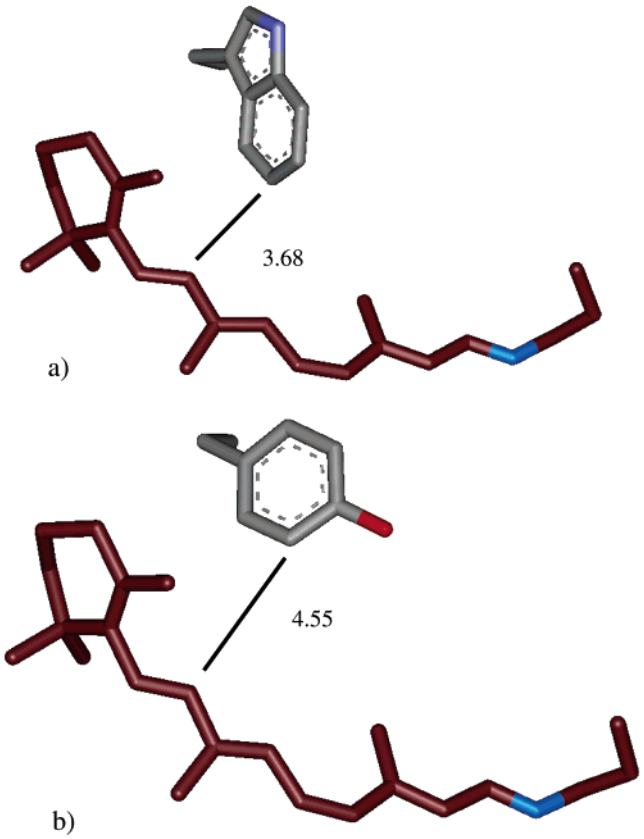

Figure 6. The polarizable aromatic side chain in the immediate vicinity of the PSB retinal is (a) Trp265 in the green (shown) and red opsins and (b) Tyr265 in the blue opsin. In the current study, we explored the importance of the polarizability of these groups in the opsin shift. The distances between the residue and the PSB retinal are indicated (Å).

replaced with nonpolar residues in the green opsin. In particular, the conformation of Tyr261 [in red opsin (which is Phe in the green opsin)] was thought to be important in the opsin shift.[1] Rotating the OH dipole of the tyrosine by 180° leads to a calculated energy gap of 43.5 kcal/mol, virtually equivalent to that of the other conformer. There are no changes (between the red and green opsins) in the residues closest (<5 Å) to the retinal PSB that could cause differential twisting, as in the green−blue opsins. Thus, the assumption that the ligand is in the same conformation in both opsins (red and green) is somewhat reasonable. Nevertheless, we found a small role of room temperature dynamics on modulating this small energy shift, as reported in section 3.4.

The presence of dipolar residues near the Schiff base region of the retinal PSB has been suggested previously to play the predominant role in the green to blue shift.[1] However, our calculations find instead an opposite shift of −2.0 kcal/mol. Thus, we conclude that either the polarizable side chains or the twisting of the retinal must play a significant role in this particular shift, as confirmed below.

3.3. Role of Polarizable Side Chains on the Opsin Shift. As discussed in section 1, polarizable side chains in the vicinity of the retinal PSB have been implicated in modulating the absorption frequency of retinal.[3,9] In particular, there is a Trp265 within the binding site of the retinal PSB in the green and red opsins, whereas the blue opsin has Tyr265 (Figure 6) in this location. Thus, it is possible that differential effects due to these polarizable residues play a role in the 13 kcal/mol experimental shift in excitation energy between the green and blue opsins. The accuracy of HF calculations in ascertaining this particular contribution is expected to be low, as discussed in section 3.1.

TABLE 1: Calculated Excitation Energies for the QM-Treated PSB/Aromatic System *without* Protein[a]

green opsin conformation no.	energy gap (kcal/mol)	blue opsin conformation no.	energy gap (kcal/mol)
1	42.7	1	43.1
2	42.5	2	43.2
3	43.5	3	43.1
4	44.1	4	42.7
5	43.0	5	43.0
6	42.8	6	42.9
		7	42.6
		8	42.5
		9	42.8
		10	43.0
av	43.1	av	42.9

[a] Here we generated the favorable side chain conformations of the aromatic residue Trp265 using SCREAM. These results indicate that the average contribution of the Trp265 aromatic residue does not affect the excitation energy gap.

TABLE 2: Calculated Excitation Energies for the QM-Treated PSB/Aromatic System *with* Protein[a]

green opsin conformation no.	energy gap (kcal/mol)	blue opsin conformation no.	energy gap (kcal/mol)
1	44.7	1	42.2
2	44.4	2	42.2
3	45.2	3	42.0
4	45.5	4	41.7
5	44.9	5	42.1
6	44.6	6	42.0
		7	41.8
		8	41.6
		9	41.8
		10	42.0
av	44.9	av	41.9

[a] The conformations of the aromatic residue 265 were generated using SCREAM. We find that the energy gaps differ by an average shift of −3.0 kcal/mol.

Even so, for completeness, our calculations exploring this contribution are presented here.

To examine this contribution, we used SCREAM (side chain conformation sampling procedure) to find the best side chain rotamer placement on the basis of the Dreiding FF scoring (with explicit hydrogen bond terms) using a 1.0 Å resolution side chain rotamer library with 1478 rotamers. SCREAM also uses MPSim to evaluate the energy of interaction of each side chain rotamer with the ligand and the rest of the protein; subsequently the rotamers can be scored and the top rotamers selected.

Then we performed QM calculations including only the retinal PSB and residue 265. This allows for differential polarizability contributions. The resulting excitation energy gaps shown in Table 1 are virtually equivalent. Thus, in these calculations, the polarizability of the aromatic residues in the presence of the retinal PSB does not lead to an opsin shift independent of the rest of the protein. This is likely due to the lack of explicit electron correlation within the QM region, as discussed earlier. This leaves the test of how the polarizabilities of these aromatic groups change within the protein in our calculations.

To determine this role of polarizability, both the aromatic side chain and retinal PSB were treated with QM in a QM/MM calculation. The results are shown in Table 2. We find a shift of −3.0 kcal/mol, opposite in direction from the expected value. Part of this shift is due to the presence of the protein dipolar residues. This component was obtained from QM calculations of the retinal PSB using the MM treatment of the protein (including the aromatic side chain) in section 3.2, which led to a calculated shift of −2.0 kcal/mol. The difference in these

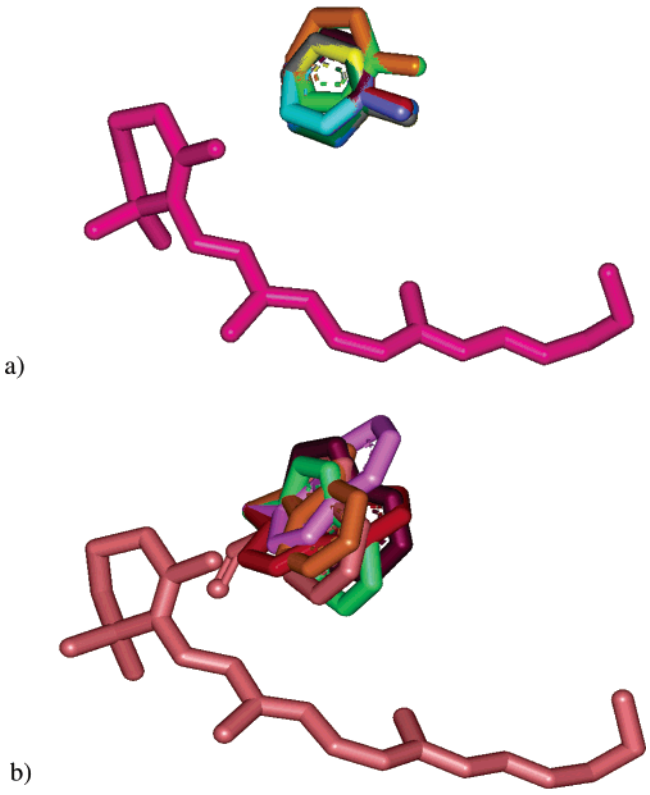

Figure 7. Conformations generated (using the Monte Carlo method of SCREAM) for the polarizable aromatic groups (a) Tyr265 and (b) Trp265 to explore the independent role of the polarizability of this residue. Note the general orientation of the Tyr conformation (as opposed to that of the bulkier Trp) along the length of the dipolar polyene chain.

numbers [−3.0 − (−2.0) = −1.0] may be attributed to the polarizability of the aromatic residue in the presence of the protein, a relatively minor contribution. The polarizability of the aromatic group within the protein should depend on the orientation with respect to the dipole of the polyene chain and dipolar residues of the protein. We determined these orientations from Monte Carlo sampling, as shown in Figure 7a. This reorientation along the PSB polyene is influenced by protein side chains, which make the orientation more difficult to achieve for the bulkier Trp in the green opsin (Figure 7b). In addition, the presence of acidic groups on helix 2 provides a dipolar environment which polarizes the Trp aromatic ring in the center of the polyene chain (not along the polyene chain length as in the case of Tyr in the blue opsin); this serves to increase the excitation energy gap by destabilizing the excited state of the PSB, which has more positive charge in this middle region (as shown in Figure 8).

We attribute the contribution of −1.0 kcal/mol to the polarization of the residue at position 265 in response to the protein's dipolar residues (in particular the acidic residues on helix 2) and not the dipole of the retinal PSB. To determine the role of the polarization of the residue at position 265 by the retinal PSB dipole may require DFT/MM to account for electron correlation in the QM region

Since this polarization accounts for only −1.0 kcal/mol of the opsin shift from green to blue, we must ask what the additional contributor to this +13.3 kcal/mol opsin shift is. To search for such contributions, we explored how the twisting of the retinal due to fluctuations at room temperature might lead to protein interactions that might contribute to the opsin shift.

3.4. MD Simulations on Opsin Complexes with the QM-Fitted Force Field for PSB. Using the modified Dreiding force

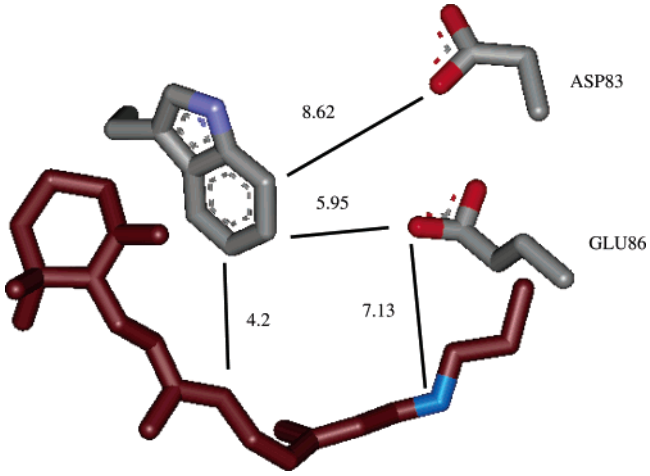

Figure 8. Acidic groups of helix 2 shown in relation to the polarizable aromatic group Trp265 in the green opsin. The presence of these groups in the protein is important in controlling the polarizability of the Trp residue. The distances between the residues and the PSB retinal are indicated (Å).

field parameters fit to the corresponding QM values for retinal PSB (as discussed in section 2.4), we carried out TVN MD (all atoms movable, except the terminal carbon of retinal PSB, to prevent the molecule from moving out of its binding pocket) for 100 ps. Single-point QM/MM calculations (all atoms fixed) were performed on snapshots every 2 ps (with QM treatment for retinal PSB). The calculated CSS to triplet energy gaps, or VEE(calcd-ts), from these 50 structures were obtained. Gaussian functions were fit to these sets of data using Bestfit v4.5.5. The absolute values of these data sets were corrected with the red peak as a baseline (using the experimental value of 560 nm for the red peak) for visual purposes. The histograms for the corrected values for VEE(calcd-ts), or VEE(calcd-ts-rel), are overlaid (red, green, and blue opsins) for comparison in Figure 9a. The Gaussian curves (fitted to the data sets) are shown in Figure 9b. The peaks of these Gaussian curves correspond to corrected energy gaps of 51.1 (560 nm), 53.3 (536 nm), and 56.7 (504 nm) kcal/mol for the red, green, and blue opsins, respectively (uncorrected values are 37.7, 40.0, and 43.3 kcal/mol). The experimental absorption spectra of the three opsin complexes from Nathans[28] are shown in Figure 9c.

The calculated red to green shift is 2.3 kcal/mol (compared to the value of 1.4 kcal/mol obtained in section 3.2 without room temperature effects of the retinal/protein conformational change), which is comparable to the 2.9 kcal/mol from experiment. Thus, the role of the dipolar residues (shown in Figure 5) (and to a lesser extent retinal twisting) in the room temperature simulation predominates over the 100 ps of MD. The Gaussian curves for VEE(calcd-ts-rel) in Figure 9b demonstrate correspondence to the experimental line shape in Figure 9c, with a wider extension in the red region. The discrepancy between the calculated and experimental absorption peaks may be attributed to (1) the role of the polarizable aromatic side chains and (2) the need to treat cavities around dipolar residues with explicit solvation.

Since the polarizable side chain at position 265 is the same in both red and green opsins, we expect that the error due to the role of these residues would be small compared to that in the case of the green−blue opsins.

Our study did not include explicit solvation, which may be important[12] in the region around the Schiff base. We excluded explicit solvation in studying to allow direct interpretation of the factors discussed in section 1.

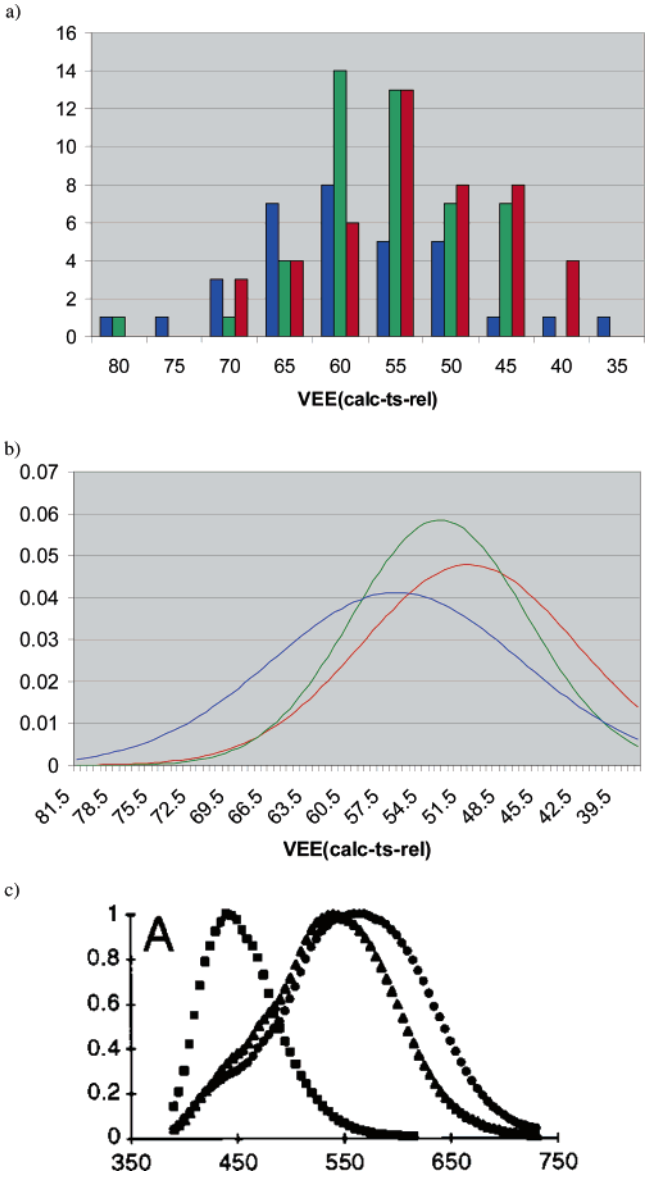

Figure 9. (a) Histograms of the VEE(calcd-ts-rel) excitation energies (using one-point QM) for the snapshots obtained from molecular dynamics for 100 ps at room temperature. (b) Also shown are the Gaussian curve fits to these histograms. (c) The experimental absorption spectra (as reported by Nathans[20]) of the three opsins are also shown.

The calculated green to blue shift is 3.4 kcal/mol, which can be compared with the 13.3 kcal/mol from experiment. This calculated shift is likely due to the greater steric interaction of the bulkier Trp in the green opsin, causing greater twisting of the PSB at room temperature (as shown in Figure 11). This greater twisting causes decreased π overlap and thus greater destabilization of the ground-state electronic state. This dominates the calculated decrease in the excitation energy gap of the green opsin by 3.4 kcal/mol as compared to that of the blue opsin. This simulation includes the effects of both the dipolar residues and retinal PSB twisting. To estimate the independent contribution of retinal PSB twisting, one can subtract the value of -2.0 obtained in section 3.2 to yield $3.4 - (-2.0) = 5.4$ kcal/ mol. Thus, retinal PSB twisting is a significant contributor in green-shifting the green opsin, whereas the dipolar residues surprisingly contribute by blue-shifting the green opsin as a fine adjustment.

The calculated absorption curves for the blue opsin are wider than the experimental spectra. This may be most likely due to the larger error in the 3D structure of the blue opsin homology model in the vicinity of the retinal PSB (as compared to those of the green and red opsins). This larger error in original protein structure would presumably lead to a more destabilized structure prone to variations in energy calculation, especially in room temperature dynamics.

There remains a large discrepancy of $13.3 - 3.4 = 9.9$ kcal/mol in the green−blue shift. Most of this difference may be due to the effect of the polarizable residues on the retinal PSB, with an induced electron density on the aromatic residue (due to the retinal PSB dipole change), which in turn may affect the stability of the retinal PSB dipole. This may be due partly to electron correlation and partly to changes in the solvation around the cavities near the dipolar residues, as discussed above for the red to green shift. To further explore the role of polarizable residues on the opsin shift in these MD structures, we carried out CIS calculations on these snapshots.

3.5. CIS Method Applied to MD-Generated Structures. As discussed in section 2.5, complexes of local residues were obtained from the MD snapshots. These complexes of local residues included retinal PSB, residue 265, and/or residue 113. CIS calculations were carried out on these small complexes.

Figure 10a shows that the CIS excitation energy [VE(CIS)] has a bimodal distribution for the local_PSB_265 complexes. Inclusion of the counterion 113 to generate the local_PSB_265_113 complexes leads to a normal distribution for both green and blue opsins, as shown in Figure 10b. The Gaussian fit (in Figure 10c) to this (local_PSB_265_113) data leads to peaks at 52.6 and 59.2 kcal/mol (for the green and blue opsin cases, respectively). This calculated opsin shift of 6.6 kcal/mol underscores the independent role of the polarizable residues in the opsin shift using the CIS level of theory. It should be noted that this value may include some contribution from the polyene twisting and some dipolar residues (as indicated in Table 3). When applying the corrections from HF level of theory, the independent contribution from the polarizable residues is $6.6 - (-2.0) - 5.4 = 3.2$ kcal/mol.

4. Conclusion

To address the fundamental question of how opsins modulate the frequency of light absorbed by a bound chromophore, we built structures of the three human color opsins on the basis of the homology to the bovine rhodopsin crystal structure. In addition, we used QM and hybrid QM/MM techniques in conjunction with MD to determine the roles of these opsin structures in modulating the frequency of maximal absorption of light by the bound retinal PSB.

We found that the predominant contributor to the red to green opsin shift (2.3 kcal/mol calculated vs 2.9 kcal/mol experimental) is the effect of the protein dipolar residues on the retinal PSB. In addition, the calculated absorption spectra demonstrate similar trends in line shape, including a wider extension of the red spectra in the red range. These results point to the utility of this QM/MM/MD approach in obtaining absorption spectra, as found by Damjanovic et al.[13]

We found that an important factor in the green to blue opsin shift (13.3 kcal/mol experimental) is twisting of the retinal PSB as a result of a bulkier aromatic side chain at position 265 (Trp in the green opsin as opposed to Tyr in the blue opsin), accounting for a calculated 3.4 kcal/mol of the green−blue shift. This twisting destabilizes the ground-state π system of the polyene chain of PSB, thus decreasing the excitation energy gap in the green opsin as compared to the blue opsin. This suggests that an additional bulky group in the vicinity of the

TABLE 3: Summary of Energetic Contributions (kcal/mol) to the Excitation Energy Shifts across the Three Opsins[a]

	red to green	green to blue
polyene chain twisting	negligible	5.4
dipolar residues	2.3	−2.0
polarizable residues	negligible	−1.0 (without electron correlation between QM regions) 6.6 kcal/mol (with the CIS level of theory, when the corrections for twisting and dipolar residues are applied from HF level of theory, the polarizable residues contribute 3.2 kcal/mol)
total shift computations	2.3	3.4 (excluding the calculated effect of polarizable residues) 10.0 (including the calculated effect of polarizable residues at the CIS level of theory; when corrections from HF level are applied as above, the shift is 6.6)
total shift experiment	2.9	13.3

[a] A positive value indicates a blue shift, whereas a negative value indicates a red shift. The contributions by the polyene twisting and polarizable residues in the red to green shifts are assumed to be negligible since the binding site residues are very similar.

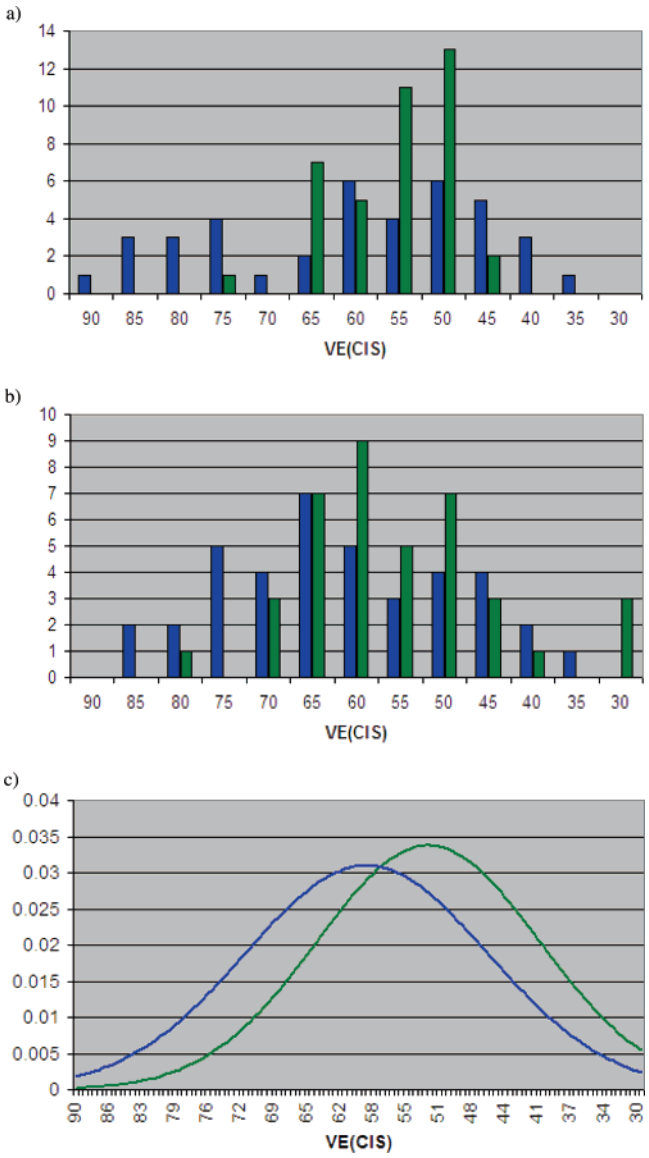

Figure 10. (a) Histograms of the VE(CIS) excitation energies (using one-point QM-CIS) for the local_PSB_265 complexes obtained from the molecular dynamics snapshots. Note the bimodal distribution for the blue opsin complexes without residue 113. (b) Also shown are the histograms of the VE(CIS) excitation energies (using one-point QM-CIS) for the local_PSB_265_113 complexes. Note the normal distributions for these complexes with counterion 113. (c) The Gaussian fit to the data in (b) is shown.

PSB in the green opsin (e.g., mutation at position 268 from the Tyr to a Trp) would further red shift the chromophore (assuming the protein folds properly and the PSB binds close to the same binding site).

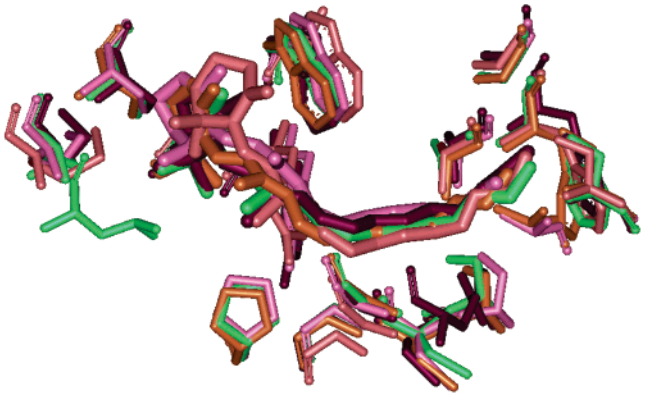

Figure 11. Sample snapshots from the 100 ps molecular dynamics room temperature simulation of the green opsin complex in the vicinity of the PSB retinal. The PSB retinal twists significantly (from −8.2° to +13.3° at the 11-*cis* bond for the snapshots above) during the simulation, due primarily to the bulky Trp265 in the immediate vicinity. This twisting is responsible for the majority of the calculated green to blue opsin shift.

The discrepancy between experimental and calculated values leads us to believe that the inherent polarizability of the aromatic side chains plays a major role in the opsin shift. Polarization of the Trp aromatic side chain is important in the green opsin, effectively decreasing the excitation energy gap in the green opsin. The dipolar residues in the protein also make an independent and unexpected (green-shifting the blue opsin) contribution of −2.0 kcal/mol in the green to blue opsin shift. Using the CIS level of theory to determine the effect of the polarizable residues, we find a shift of 6.6 kcal. A summary of these contributions is given in Table 3.

Improved understanding of this photoexcitation event may lead to various applications. This atomic-based mechanism for the spectral shifts could be used to develop proteins (or a synthetic analogue of a peptide) designed to modulate the frequency of light absorbed by bound chromophores. This could be used in medical imaging diagnostic tests, for example, in the detection of chromophoric toxins within the body. In thin sections from surgical specimens, the designed protein would be able to bind to the toxin and thus determine its localization within that specimen (on the basis of controlled absorption properties). This would advance understanding of the pathophysiology of the toxins as well as monitor the progression of disease in patients.

Conversely, the chromophore could be modified to interact specifically with a native protein to absorb at a specific frequency, which could aid in detecting overexpressed protein products for the purpose of localizing cancers (or amyloidosis, prion disease) within the body. By a manner similar to that above, surgical specimens could be histochemically analyzed for localization of the chromophore to sites of overproduction

of a certain protein (a promising alternative to the use of monoclonal antibodies with fluorescent tags).

Acknowledgment. Partial support was provided by NIH (MH073910-01). The computational facilities were provided by ARO-DURIP and ONR-DURIP grants. The facilities of the Materials and Process Simulation Center are also supported by the ONR, the DOE, the NSF, the MURI-ARO, the MURI-ONR, Chevron, Intel, Berlex Biopharma, and Aventis Pharma.

Supporting Information Available: Three human opsin structures obtained and used in this study in PDB format, with counterions included in the structures. This material is available free of charge via the Internet at http://pubs.acs.org.

Note Added after ASAP Publication. This article was released ASAP on July 29, 2006. Table 3 and the Acknowledgment has been revised. The correct version was posted on August 7, 2006.

References and Notes

(1) Kochendoerfer, G. G.; Lin, S. W.; Sakmar, T. P.; Mathies, R. A. *Trends Biochem. Sci.* **1999**, *24*, 300−305.

(2) Lin, S. W.; Kochendoerfer, G. G.; Carroll, K. S.; Wang, D.; Mathies, R. A.; Sakmar, T. P. *J. Biol. Chem.* **1998**, *273*, 24583−24591.

(3) Houjou, H.; Inoue, Y.; Sakurai, M. *J. Am. Chem. Soc.* **1998**, *120*, 4459−4470.

(4) van der Steen, R.; Biesheuvel, P. L.; Mathies, R. A.; Lugtenburg, J. *J. Am. Chem. Soc.* **1986**, *108*, 6410−6411.

(5) Sakmar, T. P.; Franke, R. R.; Khorana, H. G. *Proc. Natl. Acad. Sci. U.S.A.* **1991**, *88*, 3079−3083.

(6) Yan, B.; Spudich, J. L.; Mazur, P.; Vunnam, S.; Derguini, F.; Nakanishi, K. *J. Biol. Chem.* **1995**, *270*, 29668−29670.

(7) Lugtenburg, J.; Muradin-Szweykowska, M.; Harbison, G. S.; Smith, S. O.; Heeremans, C.; Pardoen, J. A.; Herzfeld, J.; Griffin, R. G.; Mathies, R. A. *J. Am. Chem. Soc.* **1986**, *108*, 3104−3105.

(8) Mathies, R.; Stryer, L. *Proc. Natl. Acad. Sci. U.S.A.* **1976**, *73*, 2169−2173.

(9) Torii, H. *J. Am. Chem. Soc.* **2002**, *124*, 9272−9277.

(10) *Jaguar v4.0*; Schrodinger, Inc.: Portland, OR.

(11) Spudich, J. L.; McCain, D. A.; Nakanishi, K.; Okabe, M.; Shimizu, N.; Rodman, H.; Honig, B.; Bogomolni, R. A. *Biophys. J.* **1986**, *49*, 479−483.

(12) Rajamani, R.; Gao, J. *J. Comput. Chem.* **2001**, *23*, 96−105.

(13) Damjanovic, A.; Kosztin, I.; Kleinekathofer, U.; Schulten, K. *Phys. Rev. E* **2002**, *65*, 031919.

(14) Palczewski, K.; Kumasaka, T.; Hori, T.; Behnke, C.; Motoshima, H.; Fox, B.; Trong, I.; Teller, D.; Okada, T.; Stenkamp, R.; et al. *Science* **2000**, *289*, 739−745.

(15) Trabanino, R. J.; Hall, S. E.; Vaidehi, N.; Floriano, W. B.; Kam, W. T.; Goddard, W. A. *Biophys. J.* **2003**, *86*, 1904−1921.

(16) Stenkamp, R. E.; Filipek, S.; Driessen, C. A. G. G.; Teller, D. C.; Palczewski, K. *Biochim. Biophys. Acta* **2002**, *1565*, 168−182.

(17) Thompson, J. D.; Higgins, D. G.; Gibson, T. J. *Nucleic Acids Res.* **1994**, *22*, 4673−4680.

(18) Bower, M.; Cohen, F. E.; Dunbrack, R. L. *J. Mol. Biol.* **1997**, *267*, 1268−1282.

(19) Mayo, S. L.; Olafson, B. D.; Goddard, W. A., III. *J. Phys. Chem.* **1990**, *94*, 8897−8909.

(20) MacKerell, A. D.; Bashford, D.; Bellott, M.; Dunbrack, R. L.; Evanseck, J. D.; Field, M. J.; Fischer, S.; Gao, J.; Guo, H.; Ha, S.; et al. *J. Phys. Chem. B* **1998**, *102*, 3586−3616.

(21) Lim, K.-T.; Brunett, S.; Iotov, M.; McClurg, R. B.; Vaidehi, N.; Dasgupta, S.; Taylor, S.; Goddard, W. A., III. *J. Comput. Chem.* **1997**, *18*, 501−521.

(22) Murphy, R. B.; Philipp, D. M.; Friesner, R. A. *J. Comput. Chem.* **2000**, *21*, 1442−1457.

(23) *Turbomole v5.8*; University of Karlsruhe: Karlsruhe, Germany, 2004.

(24) Muller, R. Chemistry Thesis, California Institute of Technology, Pasadena, CA, 1994.

(25) Lopez, C. S.; Faza, O. N.; Estevez, S. L.; DeLera, A. R. *J. Comput. Chem.* **2005**, *27*, 116−123.

(26) Olson, R. M.; Varganov, S.; Gordon, M. S.; Metiu, H.; Chretien, S.; Piecuch, P.; Kowalski, K.; Kucharski, S. A.; Musial, M. *J. Am. Chem. Soc.* **2005**, *127*, 1049−1052.

(27) Coussan, S.; Ferro, Y.; Trivella, A.; Rajzmann, M.; Roubin, P.; Wieczorek, R.; Manca, P.; Piecuch, P.; Kowalski, K.; Wloch, M.; Kucharski, S. A.; Musial, M. *J. Phys. Chem. A* **2006**, *110*, 3920−3926.

(28) Schmidt, M. W.; Baldridge, K. K.; Boatz, J. A.; Elbert, S. T., Gordon, M. S., Jensen, J. H.; Koseki, S.; Matsunaga, N.; Nguyen, K. A.; Su, S. J.; Windus, T. L. *J. Comput. Chem.* **1993**, *14*, 1347−1363.

(29) Nathans, J. *Neuron* **1999**, *24*, 299−312.